PHYSICAL REVIEW B **81**, 155315 (2010)

Trap density of states in small-molecule organic semiconductors: A quantitative comparison of thin-film transistors with single crystals

Wolfgang L. Kalb,* Simon Haas, Cornelius Krellner, Thomas Mathis, and Bertram Batlogg
Laboratory for Solid State Physics, ETH Zurich, 8093 Zurich, Switzerland
(Received 5 February 2010; revised manuscript received 25 March 2010; published 20 April 2010)

We show that it is possible to reach one of the ultimate goals of organic electronics: producing organic field-effect transistors with trap densities as low as in the bulk of single crystals. We studied the spectral density of localized states in the band gap [trap density of states (trap DOS)] of small-molecule organic semiconductors as derived from electrical characteristics of organic field-effect transistors or from space-charge-limited current measurements. This was done by comparing data from a large number of samples including thin-film transistors (TFT's), single crystal field-effect transistors (SC-FET's) and bulk samples. The compilation of all data strongly suggests that structural defects associated with grain boundaries are the main cause of "fast" hole traps in TFT's made with vacuum-evaporated pentacene. For high-performance transistors made with small-molecule semiconductors such as rubrene it is essential to reduce the dipolar disorder caused by water adsorbed on the gate dielectric surface. In samples with very low trap densities, we sometimes observe a steep increase in the trap DOS very close (<0.15 eV) to the mobility edge with a characteristic slope of 10–20 meV. It is discussed to what degree band broadening due to the thermal fluctuation of the intermolecular transfer integral is reflected in this steep increase in the trap DOS. Moreover, we show that the trap DOS in TFT's with small-molecule semiconductors is very similar to the trap DOS in hydrogenated amorphous silicon even though polycrystalline films of small-molecules with van der Waals-type interaction on the one hand are compared with covalently bound amorphous silicon on the other hand.

DOI: 10.1103/PhysRevB.81.155315 PACS number(s): 73.20.Hb, 73.61.Ph, 73.20.At, 85.30.De

I. INTRODUCTION

Organic semiconductors are envisioned to revolutionize display and lighting technology. The remaining engineering-related challenges are being tackled and the first products are commercially available already. To guarantee a sustainable market entry, however, it is important to further deepen the understanding of organic semiconductors and organic semiconductor devices.[1] Electronic trap states in organic semiconductors severely affect the performance of such devices. For organic thin-film transistors (TFT's), for example, key device parameters such as the effective charge mobility, the threshold voltage, the subthreshold swing as well as the electrical and environmental stability are considerably influenced by trap states at the interface between the gate dielectric and the semiconductor. Trap states in organic semiconductors have been studied for several decades.[2] Although the first organic field-effect transistors emerged in the 1980s, (polymeric semiconductors: Ref. 3, small-molecule organic semiconductors: Ref. 4) it is only recently, that trap states in organic field-effect transistors are a subject of intense scientific investigation (Refs. 5–7 and references therein).

The present study is focused on trap densities in small-molecule organic semiconductors. These solids consist of molecules with loosely bound π electrons. The π electrons are transferred from molecule to molecule and, therefore, are the source of charge conduction. Small-molecule organic semiconductors tend to be crystalline and can be obtained in high purity. Typical materials are oligomers such as pentacene, tetracene or sexithiophene but this class of materials also includes e.g., rubrene, C_{60} or the soluble material TIPS pentacene (Ref. 8).

Trap densities are often given as a volume density thus averaging over various trapping depths. The spectral density of localized states in the band gap, i.e., the trap densities as a function of energy [trap density of states (trap DOS)], gives a much deeper insight into the charge transport and device performance. In this paper we compare, for the first time, the trap DOS in various samples of small-molecule organic semiconductors including thin-film transistors (TFT's) where the active layer generally is polycrystalline and organic single crystal field-effect transistors (SC-FET's). These data are also compared with the trap DOS in the bulk of single crystals made of small-molecule semiconductors. It turns out that it is this comparison of trap densities in TFT's, SC-FET's and in the bulk of single crystals that is particularly rewarding.

The trap DOS in organic semiconductors can be derived from a number of different experimental techniques, including measurements of electrical characteristics of field-effect transistors, space-charge-limited current (SCLC) measurements, capacitance measurements, Kelvin-probe, thermally stimulated currents, time of flight, electron spin resonance, photoquenching rate and ultraviolet photoelectron spectroscopy (e.g., Refs. 9–14). For the present study, we focus on the trap DOS as derived from electrical characteristics of organic field-effect transistors or from SCLC measurements of single crystals.

We begin with a brief discussion of charge transport in small-molecule semiconductors followed by a summary of the current view of the origin of trap states in these materials. After a comparison of different methods to calculate the trap DOS from electrical characteristics of organic field-effect transistors we are eventually in a position to compile, compare and discuss trap DOS data.

II. CHARGE TRANSPORT IN SMALL-MOLECULE ORGANIC SEMICONDUCTORS

Even in ultrapure single crystals made of small-molecule semiconductors, the charge transport mechanism is still controversial. The measured mobility in ultrapure crystals increases as the temperature is decreased according to a power law $\mu_0 \propto T^n$.[15] This trend alone would be consistent with band transport. However, the mobilities μ_0 at room temperature are only around 1 cm^2/Vs and the estimated mean free path thus is comparable to the lattice constants. It has often been noticed that this is inconsistent with band transport.[15]

Since the molecules in the crystal have highly polarizable π orbitals, polarization effects are not negligible in a suitable description of charge transport in organic semiconductors. Holstein's polaron band model considers electron-electron interactions and the model has recently been extended.[16–18] With increasing temperature, the polaron mass increases. This effect is accompanied by a bandwidth narrowing and inevitably results in a localization of the charge carrier. Consequently, this model predicts a transition from band transport at low temperature to phonon-assisted hopping transport at higher temperatures (e.g., room temperature). The model may explain the experimentally observed increase in mobility with decreasing temperature and seems to be consistent with the magnitude of the measured mobilities at room temperature.

On the other hand, thermal motion of the weakly bound molecules in the solid is large compared to inorganic crystals. Such thermal motions most likely affect the intermolecular transfer integral. Indeed, Troisi *et al.* have shown that, at least for temperatures above 100 K, the fluctuation of the intermolecular transfer integral is of the same order of magnitude as the transfer integral itself in materials such as pentacene, anthracene, or rubrene.[19,20] As a consequence, the fluctuations do not only introduce a small correction, but determine the transport mechanism and limit the charge carrier mobility.[21] Clearly, the thermal fluctuations are less severe at a reduced temperature and the calculations predict a mobility that increases with decreasing temperature, according to a power law. This is in excellent agreement with the measured temperature dependence in ultrapure crystals. Moreover, the model predicts mobilities at room temperature between 0.1 and 50 cm^2/Vs, which also is in good agreement with experiment.[20,22] Recently, the theory of charge transport in organic semiconductors was revisited and it was found, that we have the simultaneous presence of bandlike transport and incoherent states that are dynamically localized by thermal disorder. Transport in these incoherent states is thus seen as an intrinsic complement to coherent bandlike transport.[23] Interestingly, the importance of thermal disorder is supported by terahertz transient conductivity measurements on pentacene crystals.[24]

In essence, the thermal motion of the molecules is expected to result in electronic trap states which would be related to the intrinsic nature of small-molecule semiconductors.[25] Clearly, trap states can also be due to extrinsic defects and these traps can completely dominate the charge transport.[9,26] For amorphous inorganic semiconductors such as amorphous silicon, the mobility edge picture has been developed (Fig. 1).[27,28] The mobility edge separates extended from localized states. The existence of extended states in amorphous silicon is attributed to the similarity of the short-range configuration of the atoms in the amorphous phase which is similar to the configuration in the crystalline phase.[28] Hopping in localized states is expected to be negligible if transport in extended states exists, i.e., we have an abrupt increase in mobility at the mobility edge. Only the charge carriers that are thermally activated to states above the mobility edge contribute to the transport of charge.

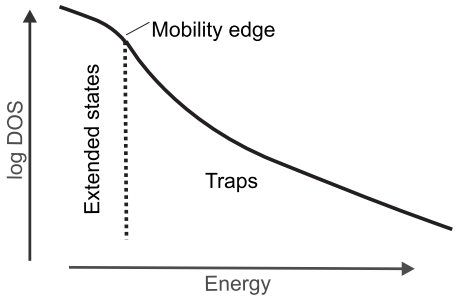

FIG. 1. Schematic representation of the mobility edge separating localized states (traps) from extended states. At the mobility edge, the mobility as a function of energy abruptly rises and only the charge carriers that are thermally activated to states above the mobility edge contribute to the charge transport.

In the following, we assume that charge transport in small-molecule semiconductors can be described by an effective transport level and a distribution of trap states below this transport level. The mobility edge model is a specific realization of this very general assumption. In a *completely* disordered material (no short-range order) all electronic states are localized.[28] The charge carriers are highly localized and hop from one molecule to the next. However, even this situation can be described by introducing an effective transport level and a broad distribution of trap states below the transport level.[29] In the following, we use the term valence-band edge. This term may generally be interpreted as the effective transport level and denotes the mobility edge in the mobility edge picture.

III. CAUSES OF TRAP STATES IN SMALL-MOLECULE ORGANIC SEMICONDUCTORS

We proceed by summarizing the current view of the microscopic origin of trap states in small-molecule semiconductors. Charge carrier traps within the semiconductor are caused by structural defects or chemical impurities. Chemical impurities may also cause a surrounding of structural defects by distorting the host lattice.[30] On the other hand, chemical impurities tend to accumulate in regions with increased structural disorder (Ref. 2) as well as at the surface of a crystal (Ref. 31). Trap states caused by the gate dielectric can become very important in organic field-effect transistors. Finally, as mentioned already, also the thermal fluctuations of the molecules are expected to result in shallow trap states within the band gap.

A. Structural defects

In the bulk of ultrapure (zone-refined) anthracene or naphthalene crystals, typical densities of vacancies (a dominant

point defect) are of the order of 10^{14}–10^{15} cm^{-3} (Ref. 2, p. 222). Vacancies are expected to be concentrated close to other structural defects due to a reduced formation energy.[2] Extended structural defects (e.g., edge dislocations, screw dislocations or low-angle grain boundaries) can be present in significant densities in organic crystals, e.g., 10^{19} cm^{-3} (Ref. 2, p.226). Therefore, extended structural defects are thought to be the main source of traps in ultrapure organic crystals.[32]

Thin films of small-molecule semiconductors are expected to have a higher density of structural defects than single crystals. These films are often polycrystalline and grain boundaries can limit the charge transport in such films. For example, measurements of sexithiophene-based transistors with SiO_2 gate dielectric and an active channel consisting of only two grains and one grain boundary show, that the transport is in fact limited by the grain boundary.[33] At the grain boundary, a high density of traps exists and the density of these traps per unit area of the active accumulation layer of the transistor is of the order of 10^{12} cm^{-2}.[33]

In the following, we focus on structural defects in vacuum-evaporated pentacene films which are of particular relevance for this work. Since pentacene films are often polycrystalline, large angle grain boundaries are expected to produce additional structural defects also in this material. The effect of grain boundaries on charge transport in pentacene films is still controversial. Atomic force measurements of ultrathin pentacene films have clearly shown, that the field-effect mobility in pentacene-based TFT's can be higher in films with smaller grains.[34] In addition, some experimental evidence indicates that there is no correlation between charge trapping and topographical features in pentacene thin films.[35] On the contrary, it has recently been shown that long-lived (energetically deep) traps that cause gate bias stress effects in pentacene-based TFT's are mainly concentrated at grain boundaries.[36] Another important cause of structural disorder in pentacene films is polymorphism. Pentacene can crystallize in at least four different structures (phases) and it is quite common that at least two of these phases coexist in pentacene thin films.[37–40] The different phases can have significant implications for the performance of pentacene-based TFT's.[41]

A theoretical study deals with in-grain defects in vacuum-evaporated pentacene films.[42] Structural defects are formed during the film growth. Upon addition of more and more "defective" molecules at a given site, the ideal crystal structure becomes energetically more and more favorable. The system eventually relaxes into the ideal crystal structure as the film continues to grow. The relaxation happens, provided that the evaporation rate is low enough and that there is enough time for relaxation.[42] In this study it is suggested that structural defects within the grains of a pentacene film that resists relaxation cannot exceed densities of 10^{16} cm^{-3}, at typical growth conditions. A structural defect can, however, influence the electronic levels of 10 surrounding molecules even if these molecules are in the perfect crystal configuration. It is concluded that grain boundaries (and not in-grain defects) are the most prominent cause of structural defects in pentacene films.[42]

On the other hand, an experimental study identifies pentacene molecules that are displaced slightly out of the molecular layers that make up the crystals.[43] By means of high impedance scanning tunneling microscopy (STM), specific defect islands were detected in pentacene films with monolayer coverage. Within the defect islands, the pentacene molecules are displaced up to 2.5 Å along the long molecular axis out of the pentacene layer with a broad distribution in the magnitude of the displacements. Electronic structural calculations show that the displaced molecules lead to traps for both electrons and holes. The maximum displacement of the pentacene molecules as seen by STM is 2.5 Å and this corresponds to a maximum trap depth of 0.1 eV.[43]

B. Chemical impurities

The best method to produce crystals of small-molecule semiconductors includes a zone refinement step in the purification procedure (Ref. 2, p. 224). Even such crystals still have a considerable impurity content. Anthracene, for example, still has an impurity content of 0.1 ppm in the best crystals, which corresponds to a volume density of $\approx 10^{14}$ cm^{-3} (Ref. 2, p. 224). Zone refinement produces organic materials of much higher purity as compared to purification by sublimation.[44] However, zone refinement can only be applied if the material can be molten without a chemical reaction or a decomposition to occur. This is not possible for many materials including tetracene or pentacene. Thus, much higher impurity concentrations are expected, e.g., in tetracene or pentacene.[44] An experimental study indicates that in tetracene single crystals the charge carrier mobility is limited by chemical impurities rather than by structural defects.[44]

The ability of a chemical impurity to act as trap depends on its accessible energy levels. In a simplistic view a hole trap forms if the ionization energy of the impurity is smaller than the ionization energy of the host material.[2] We focus on pentacene, and the center ring of the pentacene molecule is expected to be the most reactive.[45–47] An important impurity is thus thought to be the oxidized pentacene species 6,13-pentacenequinone, where two oxygen atoms form double bonds with the carbon atoms at the 6,13-positions. According to theoretical studies, pentacenequinone is expected to lead to states in the band gap of pentacene (Ref. 46 and 47). The π-electron system of pentacenequinone is smaller than that of pentacene which means that pentacenequinone has a larger band gap. It has thus been concluded that pentacenequinone predominantly acts as scattering center (Ref. 48). Repeated purification of pentacene by sublimation can result in very high mobilities in pentacene single crystals.[48] Another common impurity in pentacene is thought to be 6,13-dihydropentacene, where additional hydrogen atoms are bound both at the 6 and at the 13 position.[45]

C. Trap states due to the gate dielectric

Properties of the gate dielectric's surface such as surface roughness, surface free energy and the presence of heterogeneous nucleation sites are expected to play a key role in the growth of small-molecule semiconductor films from the vapor phase thus influencing the quality of the films.[34] Apart from growth-related effects, the sole presence of the gate

dielectric can influence the charge transport in a field-effect transistor especially because the charge is transported in the first few molecular layers within the semiconductor at the interface between the gate dielectric and the semiconductor. Thus, also FET's based on single crystals are affected, even laminated (flip-crystal-type) SC-FET's.

1. Chemical nature of the gate dielectric

The surface of the gate dielectric contains chemical groups that act as charge carrier traps. The trapping mechanism may be as simple as the one discussed above for chemical impurities. This means that the trapping depends on the specific surface chemistry of the gate dielectric but the ability of certain chemical groups on the surface of the gate dielectric to cause traps will also depend on the electronic structure of the small-molecule semiconductor. The trapping mechanism can also be seen as a reversible or irreversible electrochemical reaction driven by the application of a gate voltage.[46] Chemical groups on the surface of the gate dielectric certainly affect the transport of electrons in *n*-type field-effect transistors.[49–51]

2. Adsorbed water

Water adsorbed on the gate dielectric may dissociate and react with pentacene. One possible reaction product is 6,13-dihydropentacene. The number of impurities that are formed can depend on the electrochemical potential and would thus increase as the gate voltage is ramped up in a field-effect transistor.[46]

It has also been suggested that water causes traps by reacting with the surface of the gate dielectric. Water on a SiO_2 gate dielectric with a large number of silanol groups (-Si-OH) causes the formation of SiO^- groups and the latter groups can act as hole traps.[52]

In addition to chemical reactions involving water, water molecules may act as traps themselves just like any other chemical impurity. A polar impurity molecule leads to an electric-field dependent trap depth though.[53]

Even if a polar impurity does not lead to a positive trap depth, its dipole moment modifies the local value of the polarization energy since we have highly polarizable π orbitals in organic semiconductors. This results in traps in the vicinity of the water molecules.[53,54] The net effect is a significant broadening of the trap DOS at the insulator-semiconductor interface.[53]

3. Dielectric constant of the gate dielectric

It has been suggested that the polarity of the gate dielectric surface impedes the charge transport as described in the following.[55,56] A gate dielectric with a larger dielectric constant has a more polar surface. A more polar surface has randomly oriented dipoles which lead to a modification of the local polarization energy within the semiconductor and thus to a change in the site energies. As in the case of polar water molecules, this brings a broadening of the trap DOS. The dependence of the mobility on the dielectric constant of the gate dielectric has been observed with conjugated polymers as semiconductors (Refs. 55 and 56) and with rubrene single crystal field-effect transistors.[57] More recently, a model has been put forward to quantitatively study the effect of randomly oriented static dipole moments within the gate dielectric.[58] The model predicts a significant broadening of the trap DOS within the first 1 nm at the insulator-semiconductor interface and can explain the dependence of the mobility on the dielectric constant of the gate dielectric quantitatively.[58] However, we do not have clean surfaces in real devices. Organic transistors fabricated and measured in the common ways should have, to a varying degree, a layer of adsorbed ambient gases on the surface of the gate dielectric. In this context, it is important to realize that surfaces with a low polarity have a low-surface free energy and are thus expected to have a high water repellency. Clearly, the high water repellency leads to a reduced amount of water at the critical insulator-semiconductor interface.[56]

D. Thermal motion of the molecules

As already mentioned in Sec. II, the thermal fluctuations of the intermolecular transfer integral may be of the same order of magnitude as the transfer integral itself in small-molecule semiconductors such as pentacene, anthracene or rubrene.[19,20] A theoretical study has pointed out that the large fluctuations in the transfer integral result in a tail of trap states extending from the valence-band edge into the gap.[25] Moreover, the band tail is temperature dependent. The extension of the band tail increases with temperature due to an increase in the thermal motion of the molecules.[25] For pentacene the theoretical study predicts exponential band tails $N=N_0 \exp(-E/E_0)$ with $E_0=12.7$ meV at $T=300$ K and $E_0=6.9$ meV at $T=100$ K.

Some experimental evidence suggests that trap states due to the thermal motion of the molecules play a role in samples with a low trap density.[12,59,60]

IV. CALCULATING THE TRAP DOS FROM EXPERIMENT

Field-effect transistors are often used to measure the trap DOS. The trap DOS can be calculated from the measured transfer characteristics with various analytical methods or by simulating the transistor characteristics with a suitable computer program. In Sec. V we quantitatively compare the trap DOS from various studies in the literature with our data. Since in these studies different methods were used to derive the trap DOS, it is necessary to ensure that all these methods lead to comparable results. Analytical methods that are relevant for the comparison in Sec. V were developed by Lang *et al.* (Ref. 10), Horowitz *et al.* (Ref. 9), Fortunato *et al.* (Ref. 61), Grünewald *et al.* (Ref. 62), and Kalb *et al.* (method I: Ref. 63, method II: Ref. 7). The trap DOS as calculated with the different methods from the same set of measured data is shown in Fig. 2.[7] Clearly, the choice of the method to calculate the trap DOS has a considerable effect on the final result. The graph also contains the trap DOS obtained by simulating the transistor characteristics with a computer program developed by Oberhoff *et al.* and this may be taken as the most accurate trap DOS.[7,64] The analytical results agree to a varying degree with the simulation. Method

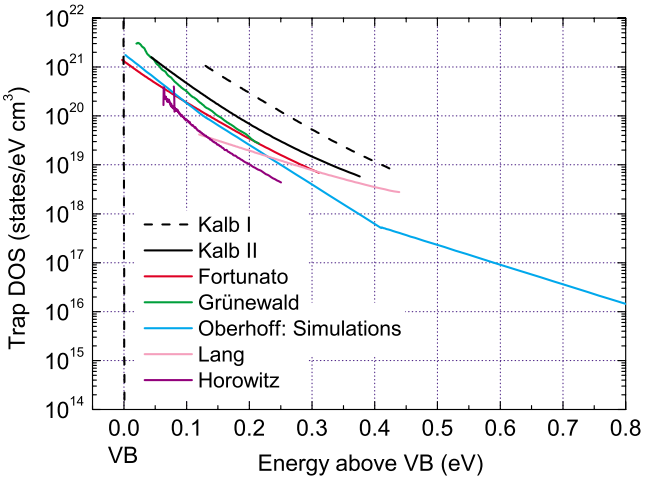

FIG. 2. (Color online) Spectral density of localized states in the band gap (trap DOS) of pentacene as calculated with several methods from the same set of transistor characteristics. The transistor characteristics were measured with a pentacene-based TFT employing a polycrystalline pentacene film and a SiO_2 gate dielectric. The energy is relative to the valence band edge (VB). The choice of the method to calculate the trap DOS has a considerable effect on the final result. Adapted from Ref. 7.

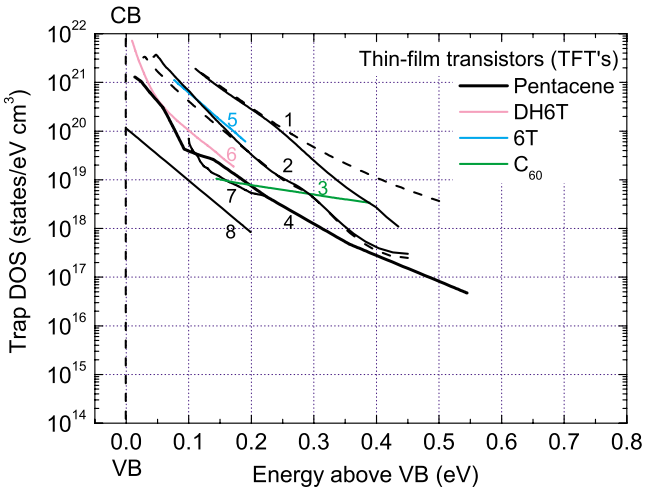

FIG. 3. (Color online) Trap DOS from thin-film transistors (TFT's) made with small-molecule organic semiconductors. Several different semiconductors, gate dielectrics and methods to calculate the trap DOS were used. Some details of the TFT fabrication are listed in Table I along with the method that was used to calculate the trap DOS and the reference of the data. Small-molecule semiconductors tend to be crystalline and can be obtained in high purity. Typical materials are oligomers such as pentacene or sexithiophene but this class of materials also includes, e.g., rubrene or C_{60}. The molecules interact by weak van der Waals-type forces and have loosely bound π electrons which are the source of charge conduction.

I by Kalb *et al.* gives a good estimate of the slope of the trap DOS but overestimates the magnitude of the trap densities which can be attributed to a neglect of the temperature-dependence of the band mobility μ_0.[7] For the method by Lang *et al.*, the effective accumulation layer thickness a is assumed to be constant (gate voltage independent). An effective accumulation layer thickness of $a=7.5$ nm is generally used. The method by Lang *et al.* leads to a significant underestimation of the slope of the trap DOS and, with an effective accumulation layer thickness of $a=7.5$ nm, to a significant underestimation of the trap densities very close to the valence-band edge (VB). These deviations need to be considered in the following analysis.

V. COMPARISON OF TRAP DOS DATA

On the one hand, trap DOS data were taken from publications by various groups that are active in the field. The data were extracted by using the Dagra software which allows to convert plotted data, e.g., in the figures of PDF files into data columns.[65] On the other hand, we also add to the following compilation unpublished data from experiments in our laboratory.

We focus on the trap DOS in small-molecule semiconductors. Since almost no data exists in the literature on the trap DOS in solution-processed small-molecule semiconductors, we almost exclusively deal with the trap DOS in vapor-deposited small-molecules. More specifically, the data are from TFT's which were made by evaporating the small-molecule semiconductors in high vacuum. The single crystals for the SC-FET's and for the measurements of the bulk trap DOS were grown by physical vapor transport (sublimation and recrystallization in a stream of an inert carrier gas).[66] Moreover, the electron trap DOS close to the conduction band edge (CB) has rarely been studied so far in small-molecule semiconductors and, with one exception, we are dealing with the hole trap DOS in the following.

A. Trap DOS from TFT's

In Fig. 3 we show the trap DOS in various TFT's made with small-molecule semiconductors. All transistors were fabricated by evaporating the organic material onto substrates comprising the gate electrode and gate dielectric and were completed by evaporating Au top contacts (TC). Details of the data are given in Table I. Apart from one exception we are dealing with hole traps that are plotted relative to the valence band edge (VB). The exception is C_{60} (data no. 3 in Fig. 3) and the electron trap densities are plotted relative to the conduction band edge (CB). In most cases, the active semiconducting layer is made of pentacene (black lines) and, in the following, we focus on these cases.

The pentacene-based transistors differ in the choice of the gate dielectric and also in the purity of the starting material (Table I). In addition, the trap densities were calculated with different methods which are also listed in Table I. The specific deviations due to the use of different methods were discussed in Sec. IV (Fig. 2). Considering these specific deviations, we can draw several conclusions from Fig. 3 and Table I: the difference in Fig. 3 between data no. 1 and data no. 2 is mainly due to the use of method I by Kalb *et al.* to obtain data no. 1 and the method by Grünewald *et al.* to obtain data no. 2. In other words, data no. 1 and data no. 2 correspond to transistors with similar trap densities. A similar

TABLE I. Thin-film transistors (TFT's) made with small-molecule organic semiconductors: details and references of the data shown in Fig. 3. The purity of the small-molecule semiconductor (starting material), the nature of the gate dielectric as well as contact effects may influence the trap DOS. The choice of the method to calculate the trap DOS has a considerable effect on the final result and is also listed.

Data no.	Semiconductor	Starting material	Gate dielectric	Contact material	Contact type	Method	Comment	Ref. data
1	Pentacene	Aldrich (purum), 2× recrystallized	SiO_2	Au	TC[a,b]	*Kalb I*	Full line: pristine sample, dashed line: after O_2 exposure	63
2	Pentacene	Aldrich (purum), 2× recrystallized	SiO_2	Au	TC[b]	*Grünewald*	Full line: pristine sample, dashed line: after aging	75
3	C_{60}		SiO_2	Au	TC	*Lang*	Electron traps, $a=7.5$ nm [c]	80
4	Pentacene	Aldrich (97%), no additional purification	PMMA[d] buffer layer on SiO_2	Au	TC	*Fortunato*		67 and 81
5	6T[e]		PMMA	Au	TC	*Horowitz*		9
6	DH6T[f]		PMMA	Au	TC	*Horowitz*		9
7	Pentacene		SiO_2	Au	TC	*Lang*	Pristine sample, $a=10$ nm	82
8	Pentacene	Aldrich (97%), no additional purification	SiO_2	Au	TC	*Völkel*[g]		83 and 84

[a]TC=top contacts.
[b]Gated four-terminal measurements.
[c]a is the constant effective accumulation layer thickness used for the calculations.
[d]Polymethylmetacrylate.
[e]Sexithiophene.
[f]Substituted dihexyl-sexithiophene.
[g]Computer simulations.

trap DOS is reasonable, because the procedure to fabricate the transistors was nominally identical in both cases (same deposition chamber, same gate dielectric, same purity of the starting material). Data no. 7 in Fig. 3 implies a rather low trap density although in that case, too, a SiO_2 gate dielectric was used (Table I). However, the use of the method by Lang *et al.* (in particular with an effective accumulation layer thickness as large as $a=10$ nm instead of $a=7.5$ nm) results in a significant underestimation of the trap DOS close to the valence band edge and data no. 7 is in fact a sample with a rather large trap density. Data no. 4 was calculated with the method by Fortunato *et al.* We consult Fig. 2 and conclude that the trap densities in this sample are indeed very low. Interestingly, the corresponding field-effect mobilities are as high as 1.2 cm^2/Vs.[67] Since this transistor was made with as-received pentacene (Aldrich, 97%, no additional purification), this low trap density is most probably not due to a lower density of chemical impurities in the pentacene film. The low trap density could be due to the polymethylmetacrylate (PMMA) surface being electrically passive in the sense that it does not cause charge carrier traps due to particular chemical groups on its surface when being combined with pentacene. We keep in mind that PMMA is considered as a hydrophilic material (water contact angle of ≈70°) and the dielectric constant is 3.5.[56,68] An alternative explanation for the low trap density is that the growth of pentacene on PMMA is exceptionally good thus leading to films with few structural defects, e.g., at grain boundaries.

B. Trap DOS from SC-FET's

In Fig. 4 we show the trap DOS in SC-FET's employing several different small-molecule semiconductors. Apart from data no. 13, all crystals were grown by physical vapor transport and were either made of pentacene or rubrene (data no. 9/10 or data no. 11/12, respectively). The single crystals in these transistors were grown separately and were then combined with the gate dielectric. This means that the gate dielectric cannot affect the growth of the organic semiconductor and can thus not be held responsible for structural disorder within the semiconductor as in the case of TFT's. For data no. 13 the crystal was grown from solution. Details

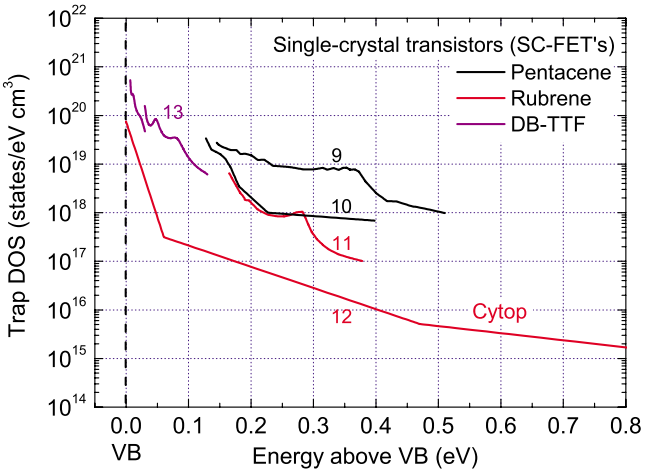

FIG. 4. (Color online) Trap DOS from single crystal field-effect transistors (SC-FET's). Different small-molecule semiconductors and gate dielectrics as well as different calculation methods were used. Details of the data are summarized in Table II. Remarkable is the very low trap density from the rubrene-based SC-FET with Cytop™ fluoropolymer gate dielectric (data no. 12).

TABLE II. Single crystal field-effect transistors (SC-FET's) made with small-molecule semiconductors: details of the data shown in Fig. 4. The purity of the starting material, the gate dielectric, contact effects and the choice of the method to calculate the trap DOS are expected to effect the magnitude and slope of the trap distribution. In each case the original study is cited.

Data no.	Semiconductor	Starting material	Gate dielectric	Contact material	Contact type	Method	Comment	Ref. data
9	Pentacene	Aldrich, 2× recrystallized	Parylene[a]	Colloidal graphite or silver	BC[b]	*Lang*	a=7.5 nm [c]	10 and 85
10	Pentacene	4× recrystallized	Parylene[a]	Colloidal graphite or silver	BC	*Lang*	a=7.5 nm	69
11	Rubrene	Aldrich, recrystallized	Parylene[a]	Colloidal graphite	BC	*Lang*		86
12	Rubrene		Cytop[d]	Au	BC	*Oberhoff* [e]		60 and 87
13	DB-TTF[f]		HMDS[g] or OTS[h] treated SiO_2 [d]	Pt or Au	BC	*Lang*	Crystals grown from solution, a=7.5 nm	88

[a]Top gate transistor structure.
[b]BC=bottom contacts (located at the insulator-semiconductor interface).
[c]a is the constant effective accumulation layer thickness used for the calculations.
[d]Bottom gate transistor structure.
[e]Computer simulations.
[f]Dibenzo-tetrathiafulvalene
[g]Hexamethyldisilazan.
[h]Octadecyltrichlorosilane.

of the SC-FET's in Fig. 4 are given in Table II. Data no. 12 stems from simulating the transistor characteristics with the computer program developed by Oberhoff *et al.* and all other trap densities were calculated with the method by Lang *et al.*

Data no. 9 and no. 10 are from pentacene-based SC-FET's and the gate dielectric is made of parylene in both cases. The same method was used to calculate the trap DOS (Lang *et al.*, a=7.5 nm) and the difference is that for data no. 9 the starting material was twice recrystallized and for data no. 10 it was 4× recrystallized. One would conclude, that chemical impurities in the single crystals have a considerable effect on the magnitude of the trap densities in SC-FET's at least in the case of pentacene.[69] The method by Lang *et al.* tends to underestimate the trap DOS, particularly closer to the valence band edge, i.e., gives lower trap densities as compared to, e.g., the trap DOS from computer simulations with the program developed by Oberhoff *et al.* (see Fig. 2). This means that data no. 12 (obtained with the method by Oberhoff *et al.*) does indeed correspond to a SC-FET with an extremely low trap density. This SC-FET is made of a rubrene single crystal which was grown in the usual way (physical vapor transport). However, the transistor employs a Cytop™ fluoropolymer gate dielectric. This shows that the specific chemistry of the gate dielectric's surface is responsible for most traps in SC-FET's. Cytop films are highly water repellent (static water contact angles up to 116°) and have a very low dielectric constant of 2.1–2.2.[70] This strongly suggests that dipolar disorder due to the presence of the gate dielectric and, more specifically, water adsorbed on the gate dielectric is a very important cause of traps in SC-FET's made with a small-molecule organic semiconductor such as rubrene. It appears that water can cause traps with a wide range of trapping depths.

C. Trap DOS in the bulk of single crystals

In Fig. 5 we show the trap DOS in the bulk of single crystals made of small-molecule semiconductors. The hole trap densities were calculated from SCLC measurements. In all cases, the crystals were grown by physical vapor transport. Some details of the data are given in Table III. Apart from one exception, all data were obtained with samples that had a sandwich-type structure (contact-crystal-contact) and temperature-dependent SCLC measurements (TD-SCLC) were used.[12,71,72] For data no. 19 however, a coplanar gap

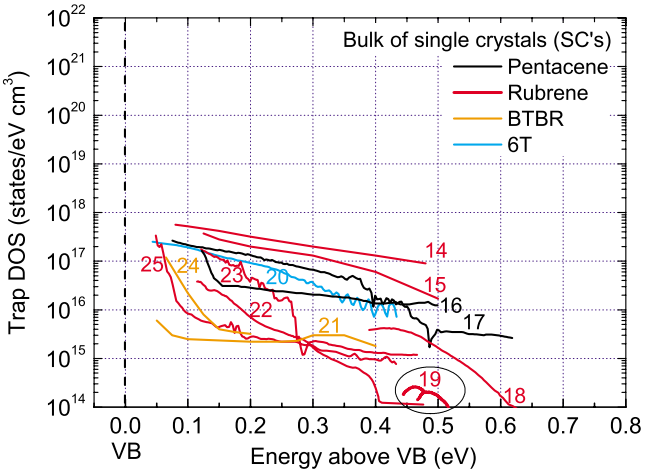

FIG. 5. (Color online) Trap DOS in the bulk of single crystals. The trap densities were calculated from SCLC measurements and the small-molecule semiconductor is, e.g., pentacene, rubrene or sexithiophene. Details of the underlying SCLC measurements and samples are summarized in Table III.

TABLE III. Bulk of single crystals made of small-molecule semiconductors: details of the trap DOS data in Fig. 5. The trap DOS was calculated from SCLC measurements in the original studies. Apart from data no. 19, TD-SCLC measurements (Temperature-dependent SCLC measurements, Refs. 12, 71, and 72) and a sandwich-type device structure were employed. In all cases Au electrodes were used.

Data no.	Semiconductor	Starting material	Ref. data
14	Rubrene	Aldrich (purum), 7× recrystallized	12
15	Rubrene	Aldrich (purum), 3× recrystallized	12
16	Pentacene	4× recrystallized	
17	Pentacene	4× recrystallized	
18	Rubrene		
19[a,b]	Rubrene		74
20	6T[c]	2× recrystallized	
21	5,11-BTBR (B)[d]	Ciba SC	59
22	Rubrene		
23	Rubrene	Aldrich (purum), 3× recrystallized	12
24	5,11-BTBR (B)	Ciba SC	59
25	Rubrene	Aldrich (purum), 3× recrystallized	12

[a]DM-SCLC (Differential-method SCLC, Refs. 73 and 74).
[b]Coplanar (gap) structure.
[c]Sexithiophene.
[d]Rubrene derivative t-butyl-tetraphenylrubrene, polymorph B.

structure (both contacts on the same side of the crystal) and differential method SCLC (DM-SCLC) was employed.[73,74] Au electrodes were used in all cases. In many cases, rubrene crystals were measured and in the following we focus on the trap DOS in the bulk of rubrene single crystals.

Data no. 15, 23, and 25 are the trap DOS in three different rubrene crystals but for all of these crystals, the starting material was 3× recrystallized. Since we have significant differences in the trap densities when comparing these crystals but the same purity of the starting material, we conclude that it is not chemical impurities but structural defects that are the main cause of traps in the bulk of rubrene crystals grown by physical vapor transport. This would be as in the case of zone-refined crystals, e.g., made of naphtalene.[15] At least, we cannot identify any clear correlation between the magnitude of the trap densities and the number of the recrystallization steps to purify the starting material. Interestingly, the highest trap densities were obtained when the rubrene crystals were grown with starting material that had been recrystallized most often (7× recrystallized, data no. 14). This further supports the dominance of structural defects in the bulk of rubrene crystals.

D. Comparison: TFT's, SC-FET's, and bulk

In Fig. 6 we show typical trap densities in TFT's (black lines), SC-FET's (red lines, gray in print version), and in the bulk of single crystals (blue lines, gray in print version). The data were selected from Fig. 3–5 as typical examples.

The trap densities in SC-FET's and in the bulk of single crystals can be much lower than the trap densities in the best TFT's. We conclude that growth-related structural defects tend to be the main cause of traps in TFT's made with small-molecule semiconductors such as pentacene. These structural defects are likely to be concentrated at grain boundaries: according to Ref. 42, in-grain structural defects cannot exceed 10^{16}–10^{17} cm^{-3} at typical growth conditions. The present study deals with "fast" traps, i.e., traps with trapping and release times much shorter than e.g., the time to measure a transistor characteristic (e.g., 1 min.). Interestingly, in the case of pentacene-based thin-film transistors, long lived and energetically deep traps (>0.5 eV from the valence-band edge) that cause gate bias stress effects are mainly located at grain boundaries as well.[36]

The trap distributions as derived from measurements of the electrical characteristics of pentacene-based TFT's have a slope of typically E_0=50–60 meV.[7] A very similar value of E_0=50 meV was determined for pentacene thin films using ultraviolet photoelectron spectroscopy.[13] This completely different technique thus confirms the use of transistor measurements to calculate the trap DOS in thin films.

When comparing the trap densities in SC-FET's with the trap densities in the bulk of single crystals, we see that the trap densities are typically lower in the bulk. However, for the rubrene-based SC-FET with the highly hydrophobic Cytop fluoropolymer gate dielectric (data no. 12 in Fig. 6) the trap densities are comparable to the trap densities in the bulk of some rubrene crystals. Consequently, bulk trap densities can be reached in organic field-effect transistors (at the insulator-semiconductor interface) if the organic semiconductor has few structural defects (e.g., single crystals, no grain boundaries) and if a suitable gate dielectric is used.

If we only consider the trap densities in Fig. 6 for energies >0.15 eV, the magnitude of the trap densities appears to be correlated with the steepness of the trap distribution. The steepest trap distributions are present in TFT's. For example, fitting data no. 2 to an exponential function $N=N_0 \exp(-E/E_0)$ yields E_0=32 meV.[75] Although the method by Grünewald *et al.* underestimates the slope to some extent (see Fig. 2), the trap DOS is significantly less steep in the bulk of organic crystals (e.g., data no. 25: E_0=180 meV, Ref. 12). At present, we do not have an explanation for this correlation.

Interestingly, in several samples a steep increase in the trap DOS very close to the valence-band edge (for energies <0.15 eV) can be observed, especially in samples with a low trap density (data no. 6, 12, 16, 24, and 25). These traps are of particular importance for the performance of organic field-effect transistors. We offer two different explanations for the steep increase in the trap DOS close to the valence-band edge. On the one hand, these traps may be the signature of thermal fluctuations of the intermolecular transfer integral.[25] The thermal motion of the small-molecules are expected to result in an exponential tail of trap states and calculations predict E_0=10–20 meV at T=300 K.[25] From experiment we have E_0=22 meV (data no. 24, Ref. 59), 11 meV (data no. 25, Ref. 12), and 11 meV (data no. 12, Ref.

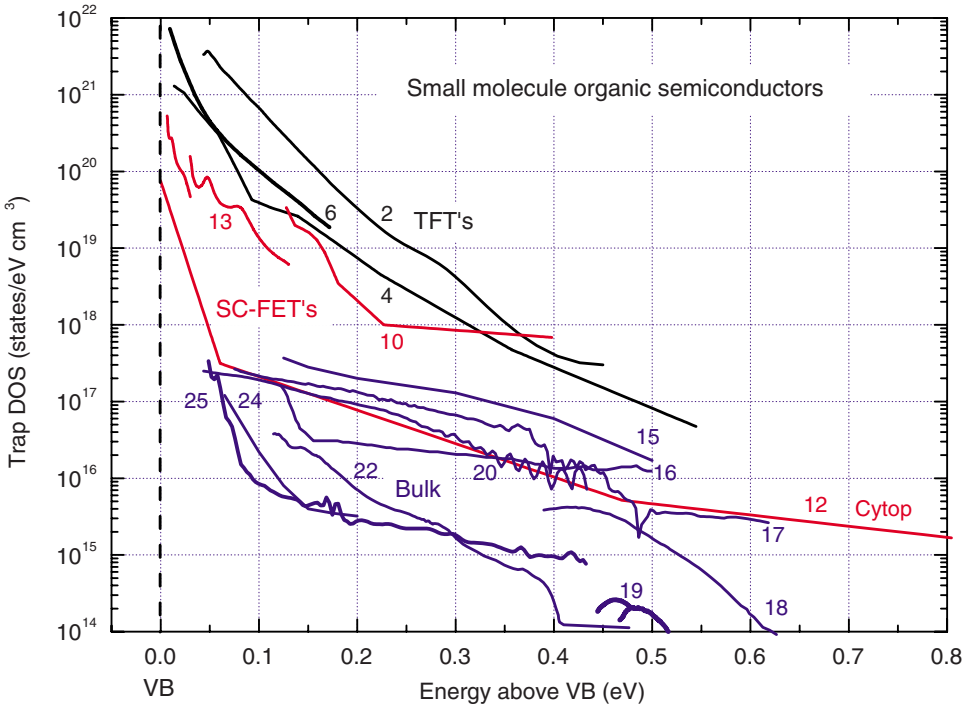

FIG. 6. (Color online) Representative trap DOS data in small-molecule organic semiconductors from thin-film transistors (TFT's, black lines), single crystal field-effect transistors (SC-FET's, red lines in online version), and in the bulk of single crystals (blue lines in online version). The data were selected from Fig. 3–5 as typical examples. The trap densities from SC-FET's can be much lower than the trap densities in the best TFT's. This strongly suggests that traps due to structural defects tend to dominate in thin films. The trap densities in the bulk of single crystals are typically lower than the trap densities from SC-FET's. Importantly, if a highly hydrophobic Cytop™ fluoropolymer gate dielectric is used, bulk trap densities can be reached in organic field-effect transistors made with small-molecule semiconductors. Thus, water adsorbed on the gate dielectric appears to be the dominant cause of traps if the semiconductor has a low density of traps due to structural defects (e.g., single crystals). A steep increase in the trap DOS very close to the valence band edge (<0.15 eV) can sometimes be observed (data no. 6, 12, 16, 24, and 25). These states are attributed to the thermal fluctuations of the intermolecular transfer integral.

60). Although the agreement between theory and experiment is compelling, we keep in mind that contact effects can be significant in organic semiconductor devices. Good electrical contacts to an organic semiconductor are difficult produce. [76] For example, contact resistances at the source and drain contact of an organic field-effect transistor are often neglected when calculating the trap DOS but can lead to an overestimation of the trap DOS particularly very close to the valence-band edge.[63] With the existing data we cannot completely rule out the possibility that the steep increase in the trap DOS is an artifact of nonideal (limiting) contacts.

E. Oxygen-related traps

We now discuss the effect of oxygen-related chemical impurities on the trap DOS. In Fig. 7 we compare the effect of oxygen exposure (in combination with light) on the trap DOS of two rubrene crystals (red and blue lines in online version, gray in print) and on the trap DOS of a pentacene thin film (black line).[12,63] For the rubrene crystals, TD-SCLC measurements were used. The peak in the trap DOS of the pentacene film was determined by employing TFT measurements and method I by Kalb *et al.*

Oxygen in combination with light results in oxygen radicals that react with the organic semiconductors. For two different organic semiconductors (pentacene and rubrene) the oxygen exposure results in a peak that is centered at the same energy, i.e., at about 0.28 eV.

For rubrene crystals, oxygen exposure leads to a sharp peak in the trap DOS. In the case of pentacene films, we have a peak with a very large width of 0.16 eV and the total concentration of states of order 10^{18} cm^{-3}.[63] The large width of the peak is thought to result from the increased local structural disorder in a thin film. The disorder modifies the on-site energy of the oxygen-affected molecules and leads to a broadening of the peak.[63]

Theoretical studies predict various types of oxygen-related defects in pentacene.[46,47,77,78] In Ref. 46 oxygen defects are discussed in which a H atom of a pentacene molecule is replaced by an oxygen atom to form a $C_{22}H_{13}O$ molecule. The oxidation at the middle ring (6 or 13 position) of the pentacene molecule is shown to be energetically most favorable.[46] The oxidation of the middle ring at one of the two sites results in the formation of two trap states in the band gap of pentacene. These are located at 0.18 and 0.62 eV above the valence band maximum.[78] In Ref. 77 other oxygen defects in pentacene are described. An example is a single oxygen intermolecular bridge where a single oxygen atom is covalently bound to the carbon atoms on the center rings of two neighboring pentacene molecules. This defect, for instance, is calculated to lead to electrically active traps at 0.33 and 0.4 eV above the valence band maximum.[77] In Ref. 47

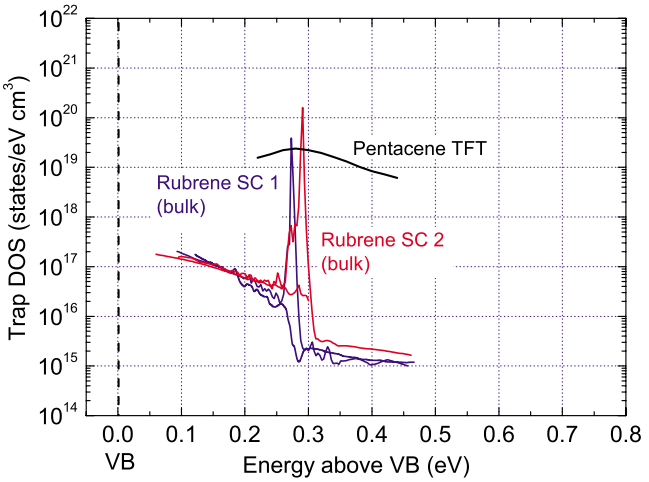

FIG. 7. (Color online) Oxygen-induced traps in rubrene and pentacene. The exposure of rubrene single crystals (SC) to oxygen in combination with light leads to a sharp peak of trap states centered at about 0.28 eV (two different samples, blue and red lines, data from Ref. 12). Exposing pentacene thin films (TFT's) to oxygen in combination with light leads to a much broader peak of trap states also centered at 0.28 eV (full black line, data from Ref. 63). For the pentacene thin film, the width of the peak is 0.16 eV and the volume density of traps as calculated from integrating the peak is 4×10^{18} cm^{-3}. The large width of the peak is thought to result from the increased local disorder in a thin film as compared to the bulk of single crystals.

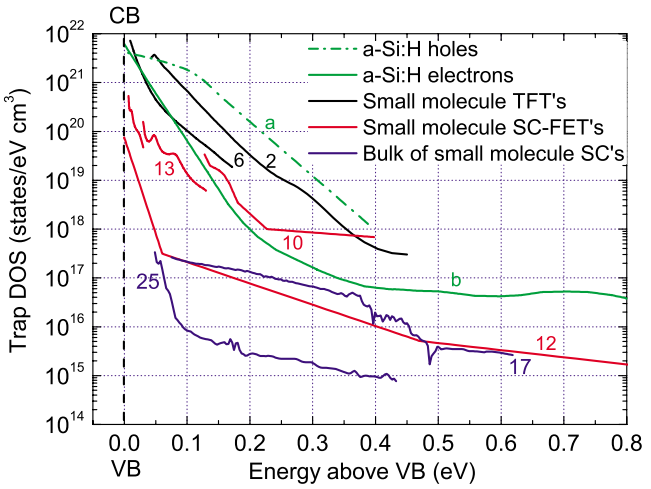

FIG. 8. (Color online) Comparison of typical trap densities in small-molecule organic semiconductors/transistors with typical trap densities in hydrogenated amorphous silicon (a-Si:H). The dashed-dotted green line (data a) is a typical distribution of hole traps in a-Si:H (energy relative to VB). The full green line (data b) marks typical electron trap densities in a-Si:H (energy relative to CB). Details of the data are given in Table IV. The hole trap DOS in a-Si:H is surprisingly similar to the hole trap DOS in small-molecule-based TFT's.

similar defects are described: an O_2 molecule may dissociate and the two oxygen atoms are bound at the 6 and 13 positions of the pentacene molecule. Calculations predict a very shallow state at 0.08 eV above the valence band maximum.[47] However, this pentacene complex can reduce its energy if one of the oxygen atoms forms a bond with a carbon atom of a neighboring pentacene molecule. This leads to acceptorlike states (0/-) at 0.29 eV above the valence band maximum.[47] Interestingly, the experimentally observed effect of oxygen exposure in combination with gate bias stress at positive gate voltages on the transfer characteristics of pentacene TFT's can be modeled by introducing a Gaussian distribution of acceptorlike states at 0.29 eV with a width of 0.1 eV and a total concentration of the order of 10^{18} cm^{-3}.[47]

F. Comparison with hydrogenated amorphous and polycrystalline silicon

It is interesting to compare the trap DOS in small-molecule organic semiconductors with the trap DOS in hydrogenated amorphous silicon (a-Si:H) and polycrystalline silicon (poly-Si). For a-Si:H, the mobility edge picture is used to describe the charge transport and trap states have been studied extensively.[28,79] The distribution of bond angles and interatomic distances in amorphous silicon (a-Si) around a mean value leads to a blurred band edge, i.e., to band tails extending into the gap. The trap densities at a given energy reflect the volume density of certain bond angles and interatomic distances. For example, a rather large deviation from the atomic configuration in the crystalline phase (from the mean value in the amorphous phase) leads to traps with energies far from the band edge. These traps are present with rather low densities since small deviations are much more likely to occur. In addition, we may have dangling bonds in a-Si acting as traps. It is well known, that hydrogenation of a-Si leads to a reduction in the trap DOS due to a passivation of dangling bonds with hydrogen.[79]

For Fig. 8 we have selected typical trap DOS data from samples with small-molecule semiconductors (data from Fig. 6). The data are compared with a typical hole trap DOS in a-Si:H (data a) and with a typical electron trap DOS in a-Si:H (data b). Details of the data are given in Table IV. In Fig. 8 we see that the hole trap DOS in TFT's with small-molecule semiconductors such as pentacene is surprisingly similar to the hole trap DOS in a-Si:H. Both the magnitude of the trap densities and the slope of the distribution are very similar.

Finally, in Fig. 9 we similarly compare data from small-molecule semiconductors with a typical hole trap DOS in poly-Si (data c) and an electron trap DOS in poly-Si (data d).

TABLE IV. Details of the trap DOS data in Fig. 8 from hydrogenated amorphous silicon (a-Si:H) and in Fig. 9 from polycrystalline silicon (poly-Si) samples.

Data	Semiconductor	Carriers	Based on	Ref. data
a	a-Si:H, good quality	Holes	Photoemission and time of flight	79 (p. 81)
b	a-Si:H	Electrons	TFT	89
c	poly-Si	Holes	TFT	90
d	poly-Si	Electrons	TFT[a]	61

[a]Calculation method: Fortunato *et al.*

The trap distribution is less steep in poly-Si as compared to the trap DOS in organic thin films such that we have higher trap densities in poly-Si far from the transport band edge.

VI. SUMMARY AND CONCLUSIONS

We compared the hole trap DOS (trap densities as a function of energy relative to the valence-band edge) in various samples of small-molecule organic semiconductors as derived from electrical characteristics of organic field-effect transistors and space-charge-limited current measurements. In particular, we distinguish between the trap DOS in thin-film transistors with vacuum-evaporated small-molecules, the trap DOS in organic single crystal field-effect transistors and the trap DOS in the bulk of single crystals grown by physical vapor transport. A comparison of all data strongly suggests that structural defects at grain boundaries tend to be the main cause of "fast" traps in TFT's made with vacuum-evaporated pentacene and supposedly also in related materials. The gate dielectric's surface is responsible for most traps in SC-FET's. We argue that dipolar disorder due to the presence of the gate dielectric and, more specifically, water adsorbed on the gate dielectric surface is the main cause of traps in SC-FET's made with a semiconductor such as rubrene. One of the most important findings is that bulk trap densities can be reached in organic field-effect transistors if the organic semiconductor has few structural defects (e.g., single crystals) and if a suitable gate dielectric is used. The highly hydrophobic Cytop™ fluoropolymer gate dielectric essentially is a gate dielectric that does not cause traps at the insulator-semiconductor interface and thus leads to organic field-effect transistors with outstanding performance.

The trap DOS in TFT's with small-molecule semiconductors is very similar to the trap DOS in hydrogenated amorphous silicon. This is surprising due to the very different nature of polycrystalline thin films made of small-molecule semiconductors with van der Waals-type interaction on the one hand and covalently bound amorphous silicon on the other hand.

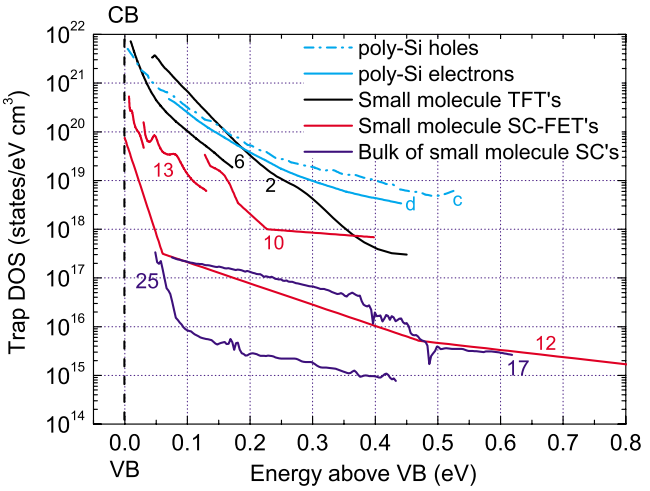

FIG. 9. (Color online) Comparison of typical trap densities in small-molecule semiconductors with typical trap densities in polycrystalline silicon (poly-Si). The dash-dotted blue line (data c) represents hole traps in poly-Si (energy relative to VB) and the full blue line (data d) marks electron traps in poly-Si (energy relative to CB). Details of the data are given in Table IV.

Although several important conclusions can be drawn from the extensive data it is clear that the present picture is not complete. More systematic studies are necessary to consolidate and complete the understanding of the trap DOS in organic semiconductors and organic semiconductor devices. The present compilation may serve as a guide for future studies.

ACKNOWLEDGMENTS

The authors thank Kurt Pernstich for a careful reading of the manuscript and for valuable suggestions. We thank Kurt Mattenberger for constant technical support.

*kalb@phys.ethz.ch

[1] N. Ueno and S. Kera, Prog. Surf. Sci. **83**, 490 (2008).
[2] M. Pope and C. E. Swenberg, *Electronic Processes in Organic Crystals and Polymers*, 2nd ed. (Oxford University Press, New York, 1999).
[3] F. Ebisawa, T. Kurokawa, and S. Nara, J. Appl. Phys. **54**, 3255 (1983).
[4] G. Horowitz, D. Fichou, X. Peng, Z. Xu, and F. Garnier, Solid State Commun. **72**, 381 (1989).
[5] D. Braga and G. Horowitz, Adv. Mater. **21**, 1473 (2009).
[6] H. Sirringhaus, Adv. Mater. **21**, 3859 (2009).
[7] W. L. Kalb and B. Batlogg, Phys. Rev. B **81**, 035327 (2010).
[8] S. K. Park, T. N. Jackson, J. E. Anthony, and D. A. Mourey, Appl. Phys. Lett. **91**, 063514 (2007).
[9] G. Horowitz, R. Hajlaoui, and P. Delannoy, J. Phys. III **5**, 355 (1995).
[10] D. V. Lang, X. Chi, T. Siegrist, A. M. Sergent, and A. P. Ramirez, Phys. Rev. Lett. **93**, 086802 (2004).
[11] O. Tal, Y. Rosenwaks, Y. Preezant, N. Tessler, C. K. Chan, and A. Kahn, Phys. Rev. Lett. **95**, 256405 (2005).
[12] C. Krellner, S. Haas, C. Goldmann, K. P. Pernstich, D. J. Gundlach, and B. Batlogg, Phys. Rev. B **75**, 245115 (2007).
[13] T. Sueyoshi, H. Fukagawa, M. Ono, S. Kera, and N. Ueno, Appl. Phys. Lett. **95**, 183303 (2009).
[14] H. Matsui, A. S. Mishchenko, and T. Hasegawa, Phys. Rev. Lett. **104**, 056602 (2010).
[15] W. Warta and N. Karl, Phys. Rev. B **32**, 1172 (1985).
[16] T. Holstein, Ann. Phys. **8**, 325 (1959).
[17] T. Holstein, Ann. Phys. **8**, 343 (1959).
[18] K. Hannewald, V. M. Stojanović, J. M. T. Schellekens, P. A. Bobbert, G. Kresse, and J. Hafner, Phys. Rev. B **69**, 075211 (2004).
[19] A. Troisi and G. Orlandi, J. Phys. Chem. A **110**, 4065 (2006).
[20] A. Troisi, Adv. Mater. **19**, 2000 (2007).

[21] A. Troisi, Mol. Simul. **32**, 707 (2006).
[22] A. Troisi and G. Orlandi, Phys. Rev. Lett. **96**, 086601 (2006).
[23] S. Fratini and S. Ciuchi, Phys. Rev. Lett. **103**, 266601 (2009).
[24] H. A. v. Laarhoven, C. F. J. Flipse, M. Koeberg, M. Bonn, E. Hendry, G. Orlandi, O. D. Jurchescu, T. T. M. Palstra, and A. Troisi, J. Chem. Phys. **129**, 044704 (2008).
[25] J. P. Sleigh, D. P. McMahon, and A. Troisi, Appl. Phys. A: Mater. Sci. Process. **95**, 147 (2009).
[26] F. Schauer, J. Appl. Phys. **86**, 524 (1999).
[27] P. W. Anderson, Proc. Natl. Acad. Sci. U.S.A. **69**, 1097 (1972).
[28] J. M. Marshall, Rep. Prog. Phys. **46**, 1235 (1983).
[29] V. I. Arkhipov, P. Heremans, E. V. Emelianova, G. J. Adriaenssens, and H. Bässler, Appl. Phys. Lett. **82**, 3245 (2003).
[30] K. H. Probst and N. Karl, Phys. Status Solidi A **27**, 499 (1975).
[31] O. D. Jurchescu, M. Popinciuc, B. J. van Wees, and T. T. M. Palstra, Adv. Mater. **19**, 688 (2007).
[32] J. Owen, G. P. Sworakowski, J. M. Thomas, D. F. Williams, and J. O. Williams, J. Chem. Soc., Faraday Trans. 2 **70**, 853 (1974).
[33] A. B. Chwang and C. D. Frisbie, J. Appl. Phys. **90**, 1342 (2001).
[34] W. Kalb, P. Lang, M. Mottaghi, H. Aubin, G. Horowitz, and M. Wuttig, Synth. Met. **146**, 279 (2004).
[35] E. M. Muller and J. A. Marohn, Adv. Mater. **17**, 1410 (2005).
[36] M. Tello, M. Chiesa, C. M. Duffy, and H. Sirringhaus, Adv. Funct. Mater. **18**, 3907 (2008).
[37] C. C. Mattheus, A. B. Dros, J. Baas, A. Meetsma, J. L. de Boer, and T. T. M. Palstra, Acta Crystallogr., Sect. C: Cryst. Struct. Commun. **57**, 939 (2001).
[38] C. D. Dimitrakopoulos and R. L. Malenfant, Adv. Mater. **14**, 99 (2002).
[39] H.-L. Cheng, Y.-S. Mai, W.-Y. Chou, L.-R. Chang, and X.-W. Liang, Adv. Funct. Mater. **17**, 3639 (2007).
[40] T. Siegrist, C. Besnard, S. Haas, M. Schiltz, P. Pattison, D. Chernyshov, B. Batlogg, and C. Kloc, Adv. Mater. **19**, 2079 (2007).
[41] H.-L. Cheng, W.-Y. Chou, C.-W. Kuo, Y.-W. Wang, Y.-S. Mai, F.-C. Tang, and S.-W. Chu, Adv. Funct. Mater. **18**, 285 (2008).
[42] S. Verlaak, C. Rolin, and P. Heremans, J. Phys. Chem. B **111**, 139 (2007).
[43] J. H. Kang, D. da Silva, J. L. Bredas, and X. Y. Zhu, Appl. Phys. Lett. **86**, 152115 (2005).
[44] J. Pflaum, J. Niemax, and A. K. Tripathi, Chem. Phys. **325**, 152 (2006).
[45] C. C. Mattheus, J. Baas, A. Meetsma, J. L. de Boer, C. Kloc, T. Siegrist, and T. T. M. Palstra, Acta Crystallogr., Sect. E: Struct. Rep. Online **E58**, o1229 (2002).
[46] J. E. Northrup and M. L. Chabinyc, Phys. Rev. B **68**, 041202(R) (2003).
[47] D. Knipp and J. E. Northrup, Adv. Mater. **21**, 2511 (2009).
[48] O. D. Jurchescu, J. Baas, and T. T. M. Palstra, Appl. Phys. Lett. **84**, 3061 (2004).
[49] M. Ahles, R. Schmechel, and H. von Seggern, Appl. Phys. Lett. **85**, 4499 (2004).
[50] L.-L. Chua, J. Zaumseil, J.-F. Chang, E. C.-W. Ou, P. K.-H. Ho, H. Sirringhaus, and R. H. Friend, Nature (London) **434**, 194 (2005).
[51] M. H. Yoon, C. Kim, A. Facchetti, and T. J. Marks, J. Am. Chem. Soc. **128**, 12851 (2006).
[52] D. Kumaki, T. Umeda, and S. Tokito, Appl. Phys. Lett. **92**, 093309 (2008).
[53] J. Sworakowski, Braz. J. Phys. **29**, 318 (1999).
[54] S. Verlaak and P. Heremans, Phys. Rev. B **75**, 115127 (2007).
[55] J. Veres, S. D. Ogier, S. W. Leeming, D. C. Cupertino, and S. M. Khaffaf, Adv. Funct. Mater. **13**, 199 (2003).
[56] J. Veres, S. Ogier, G. Lloyd, and D. de Leeuw, Chem. Mater. **16**, 4543 (2004).
[57] A. F. Stassen, R. W. I. de Boer, N. N. Iosad, and A. F. Morpurgo, Appl. Phys. Lett. **85**, 3899 (2004).
[58] T. Richards, M. Bird, and H. Sirringhaus, J. Chem. Phys. **128**, 234905 (2008).
[59] S. Haas, A. F. Stassen, G. Schuck, K. P. Pernstich, D. J. Gundlach, B. Batlogg, U. Berens, and H. J. Kirner, Phys. Rev. B **76**, 115203 (2007).
[60] K. P. Pernstich, B. Rössner, and B. Batlogg, Nat. Mater. **7**, 321 (2008).
[61] G. Fortunato, D. B. Meakin, P. Migliorato, and P. G. Le Comber, Philos. Mag. B **57**, 573 (1988).
[62] M. Grünewald, P. Thomas, and D. Würtz, Phys. Status Solidi B **100**, K139 (1980).
[63] W. L. Kalb, K. Mattenberger, and B. Batlogg, Phys. Rev. B **78**, 035334 (2008).
[64] D. Oberhoff, K. P. Pernstich, D. J. Gundlach, and B. Batlogg, IEEE Trans. Electron Devices **54**, 17 (2007).
[65] http://www.blueleafsoftware.com/.
[66] R. A. Laudise, C. Kloc, P. G. Simpkins, and T. Siegrist, J. Cryst. Growth **187**, 449 (1998).
[67] F. De Angelis, S. Cipolloni, L. Mariucci, and G. Fortunato, Appl. Phys. Lett. **88**, 193508 (2006).
[68] Y. Ma, X. Cao, X. Feng, Y. Ma, and H. Zou, Polymer **48**, 7455 (2007).
[69] W.-Y. So, D. V. Lang, V. Y. Butko, X. Chi, J. C. Lashley, and A. P. Ramirez, J. Appl. Phys. **104**, 054512 (2008).
[70] W. L. Kalb, T. Mathis, S. Haas, A. F. Stassen, and B. Batlogg, Appl. Phys. Lett. **90**, 092104 (2007).
[71] F. Schauer, S. Nešpurek, and H. Valerian, J. Appl. Phys. **80**, 880 (1996).
[72] F. Schauer, R. Novotny, and S. Nešpurek, J. Appl. Phys. **81**, 1244 (1997).
[73] S. Nešpurek and J. Sworakowski, J. Appl. Phys. **51**, 2098 (1980).
[74] D. Braga, N. Battaglini, A. Yassar, G. Horowitz, M. Campione, A. Sassella, and A. Borghesi, Phys. Rev. B **77**, 115205 (2008).
[75] W. L. Kalb, F. Meier, K. Mattenberger, and B. Batlogg, Phys. Rev. B **76**, 184112 (2007).
[76] J. E. Anthony, Angew. Chem. Int. Ed. **47**, 452 (2008).
[77] L. Tsetseris and S. T. Pantelides, Phys. Rev. B **75**, 153202 (2007).
[78] A. Benor, D. Knipp, J. Northrup, A. R. Völkel, and R. A. Street, J. Non-Cryst. Solids **354**, 2875 (2008).
[79] R. A. Street, *Hydrogenated Amorphous Silicon* (Cambridge University Press, Cambridge, 1991).
[80] N. Kawasaki, T. Nagano, Y. Kubozono, Y. Sako, Y. Morimoto, Y. Takaguchi, A. Fujiwara, C. C. Chu, and T. Imae, Appl. Phys. Lett. **91**, 243515 (2007).
[81] F. De Angelis, S. Cipolloni, L. Mariucci, and G. Fortunato, Appl. Phys. Lett. **86**, 203505 (2005).
[82] C. Vanoni, T. A. Jung, and S. Tsujino, Appl. Phys. Lett. **94**, 253306 (2009).
[83] A. R. Völkel, R. A. Street, and D. Knipp, Phys. Rev. B **66**, 195336 (2002).
[84] D. Knipp, R. A. Street, B. Krusor, R. B. Apte, and J. Ho, Proc.

SPIE **4466**, 8 (2001).
[85] V. Y. Butko, X. Chi, D. V. Lang, and A. P. Ramirez, Appl. Phys. Lett. **83**, 4773 (2003).
[86] W.-Y. So, J. M. Wikberg, D. V. Lang, O. Mitrofanov, C. L. Kloc, T. Siegrist, A. M. Sergent, and A. P. Ramirez, Solid State Commun. **142**, 483 (2007).
[87] K. P. Pernstich, Ph. D. thesis, ETH Zurich, 2007.
[88] M. Leufgen *et al.*, Org. Electron. **9**, 1101 (2008).
[89] F. Djamdji, P. G. Le Comber, R. Schumacher, P. Thomas, and K. Weber, J. Non-Cryst. Solids **97-98**, 543 (1987).
[90] H. N. Chern, C. L. Lee, and T. F. Lei, IEEE Trans. Electron Devices **41**, 698 (1994).